The optical properties of $CuPbSbS_3$-bournonite with photovoltaic applications

C. Tablero

Abstract $CuPbSbS_3$-bournonite is a quaternary semiconductor derived from the Cu–Sb–S semiconductors with numerous possibilities including optoelectronic and photovoltaic applications. An analysis focusing on the potential for solar cells is carried out starting from first-principles density functional theory with orbital-dependent one-electron potentials. In order to understand the fundamental factors responsible for the absorption, the absorption coefficients have been split into inter- and intra-species contributions. The absorption coefficients are used as a criterion for evaluating the efficiencies when this material is used to absorb sunlight at several concentrations. The results indicate their applicability in photovoltaic devices as absorbent of the solar spectrum with high energy conversion efficiency.

Keywords Optoelectronic properties · Semiconductors · Photovoltaics

1 Introduction

Of particular interest are those semiconductors with physical properties appropriate for photovoltaic applications. An important property for the semiconductors to be able to convert photon energy into useful work in an external circuit is the absorption coefficient. This property indicates the absorption threshold related to the band-gap and the sunlight absorbed as a function of the photon energy.

Many of the efforts to find new materials have focused on the synthesis and characterization of binary semiconductor systems. Part of these efforts has recently extended to exploring more complex ternary and quaternary structures. Ternary I-III-VI_2 chalcogenides, in particular $CuInSe_2$, are currently among the strongest absorbers known. However, while the overall absorption is strong, it is necessary to use rather thick films because of the weak onset absorption near the band-gap. Among the ternary materials, Cu–Sb–S-type derived semiconductors also have interesting properties as absorber materials for thin-film solar cells [1–3].

The ternary phases in this system are: Cu_3SbS_4 (famatinite), $CuSbS_2$ (chalcostibite), Cu_3SbS_3 (skinnerite and wittichenite) and $Cu_{12}Sb_4S_{13}$ (tetrahedrite). These are usually p-type semiconductors with an energy band-gap which varies from between ∼0.46 to 1.9 eV [1–11], and they frequently have a high absorption coefficient above 10^4–10^5 cm^{-1} in a wide range of the visible region [1–5]. These properties make it attractive for semiconductor-based device applications and a particularly attractive candidate for photovoltaic solar cells. The quaternary materials based on Cu–Sb–S present a wide range of opportunities through the identification and design of new and strongly absorbent materials in thin-film photovoltaics.

A quaternary compound derived from the ternary Cu–Sb–S system, $CuPbSbS_3$, could be suitable as a solar radiation absorber in solar cells. $CuPbSbS_3$ can be found in sulfide ore deposits as the mineral *bournonite* and can be prepared by direct synthesis from very pure elements obtained through a modified zone-melting method [12]. The crystal belongs to the orthorhombic class, space group $Pmn2_1$ (no. 31) [12, 13]. The experimental energy band-gap (E_g ~ 1.22 eV [12]) is closer to the optimal for single-gap

solar cells (E_g ~ 1.1 eV with maximum solar cell efficiency ~41 % [14–16]). It indicates that this compound could be suitable as a solar radiation absorber in solar cells.

Therefore, an additional knowledge of the influence of the electronic and optical properties of the absorption coefficients of the $CuPbSbS_3$-bournonite is needed in order to evaluate its potential for photovoltaic solar cells. Understanding the fundamental factors responsible for the absorption will provide new insight into refining and focusing on design pathways to reach the device level.

The identification and design of new materials require an approach beyond the classic which selects good photovoltaic absorbers exclusively on the basis of their band-gap. This approach should be based on the sunlight absorbed and the thickness of the solar cell, i.e., the absorption coefficient. The classic approximation, based on the band-gap, is in part due to the simplification of the calculation and the difficulty in obtaining absorption coefficients (theoretically or experimentally) with respect to obtaining energy band-gaps. First principles are an important and powerful complementary tool, allowing these basic properties, which are hardly accessible through experiments, to be obtained and quantified. Therefore, to achieve these objectives we present a study of these electronic and optical properties together with the fundamental aspects affecting absorption using first principles. In addition, we will analyze the potential for photovoltaics obtaining the maximum efficiencies when these materials are used as light absorbers in solar cell devices.

2 Methodology

The first-principles methodology used to obtain the electronic and optical properties is based on the density functional theory (DFT) [18, 19]. However, the spurious electron self-interactions are not dealt with properly using the standard approximations. It leads to an underestimation of both the band-gap and the bond length of weakly bound molecules and solids, and an overestimation of both the bandwidth and the binding energy, etc. In order to avoid partially the DFT self-interaction problem, an effective on-site Coulomb U (DFT + U) factor is used [20–24]. The value of U depends on the choice of the orbital subspace on which the correction is applied, on the way the orbital occupations are computed, and on the DFT + U implementation chosen [21–24]. In this work we will use the DFT + U methodology and implementation described in references [21, 22]. Furthermore, the generalized gradient approximation (GGA) from Perdew, Burke and Ernzerhof [25, 26] is used for the exchange–correlation potential, and the standard Troullier–Martins [27] pseudopotentials are adopted and expressed in the Kleinman–Bylander [28, 29] form. A numerically localized pseudoatomic orbital basis set [30] is used to expand the valence wave functions. Periodic boundary conditions, spin polarization, double-zeta with polarization localized basis sets, and the orthorhombic $Pmn2_1$ (space group 31) crystal structure with 100 and 180 special k-points in the irreducible Brillouin zone are used in all calculations.

In order to obtain the optical properties we have obtained the momentum matrix elements $p_{\mu\lambda}$ between the μ and λ bands at $\vec{k}$ points in the Brillouin zone, where $\mathbf{p} = i(m/\hbar)[H, \mathbf{r}]$. Both, the local and non-local parts of the pseudopotentials have been considered in these calculations. From energies $E_{\mu,\vec{k}}$, occupations $f_{\mu,\vec{k}}$ and momentum matrix elements $p_{\mu\lambda}$ at $\vec{k}$ points, we have obtained the complex dielectric function

$$e_2(E) \sim \frac{1}{E^2} \sum_{\lambda>\mu} \int d\vec{k} |p_{\mu\lambda}|^2 [f_{\mu,\vec{k}} - f_{\lambda,\vec{k}}] \delta(E_{\lambda,\vec{k}} - E_{\mu,\vec{k}} - E)$$

and other optical properties using the Kramers–Kronig relationships.

In addition, the momentum matrix elements can be split into $p_{\mu\lambda} = \sum_A \sum_B p^{AB}_{\mu\lambda}$, where $p^{AB}_{\mu\lambda}$ is the component that couples the basis set functions on the A and B atoms. Similarly, the absorption coefficients and other optical properties can be split into $\alpha = \sum_A \sum_B \alpha_{AB} +$ (terms involving three and four different species). α_{AA} and α_{AB} are the intra- and inter-species contributions to the total absorption coefficient.

3 Results and discussion

3.1 Structure and electronic properties

$CuPbSbS_3$-bournonite crystallizes into an orthorhombic class, $Pmn2_1$ (space group 31), with lattice parameters a = 8.153 Å, b = 8.692 Å, c = 7.793 Å, and $\alpha = \beta = \gamma = 90°$ [12, 13]. There are four different atoms (chemical species) in this structure, but nine symmetrically non-equivalent chemical species: Pb_1, Pb_2, Sb_1, Sb_2, Cu, S_1, S_2, S_3, and S_4. Figure 1 shows the details of the crystalline structure and the non-equivalent atoms. The distributions of the first shells of the nearest neighbors around the non-equivalent atoms are: Pb_1 ($S_1 + 2S_3 + S_2 + 2S_4$), Pb_2 ($S_2 + 2S_4 + 2S_4 + 2Cu + 2S_3$), Sb_1 ($S_2 + 2S_3$), Sb_2 ($S_1 + 2S_4$), Cu ($S_1 + S_2 + S_3 + S_4$), S_1 ($Pb_1 + Sb_2 + 2Cu$), S_2 ($Pb_2 + Sb_1 + 2Cu$), S_3 ($Pb_1 + Pb_2 + Sb_1 + Cu$), and S_4 ($Pb_1 + Pb_2 + Sb_2 + Cu$). Therefore, in the crystalline $CuPbSbS_3$ structure the Pb_1 and Pb_2 atoms are surrounded (at an inter-atomic distance of <3.5 Å) by six and nine S atoms, respectively. The Sb atoms have a trigonal pyramidal coordination with the

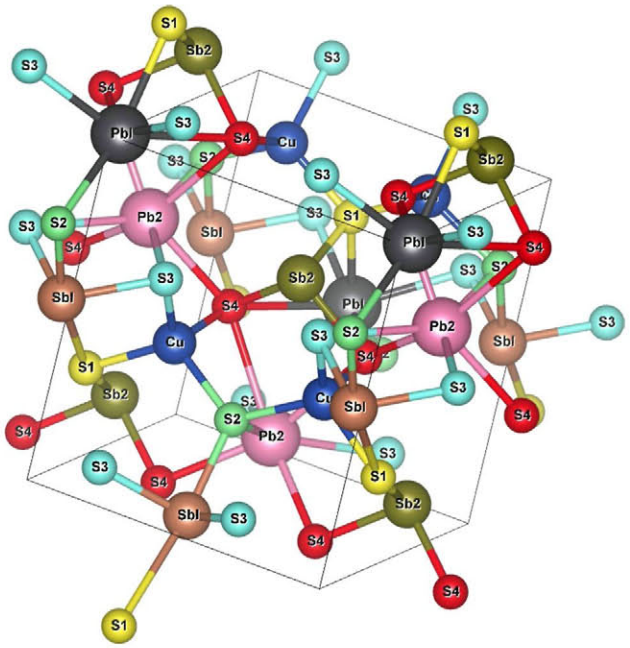

Fig. 1 Crystalline structure of the $CuPbSbS_3$-bournonite where the nine symmetrically non-equivalent chemical species (Pb_1, Pb_2, Sb_1, Sb_2, Cu, S_1, S_2, S_3, and S_4) are shown

S atoms, and these SbS_3 pyramids are isolated. The Cu atoms are tetrahedrally coordinated with slight deformations by four S atoms. The Cu tetrahedra share corners parallel to the c axis.

Compared with different compounds but with a similar composition as the $CuMS_2$ (M = Sb, Bi) [1] and the tetrahedrites [2], the Pb atoms have a very different environment than the Sb or Bi atoms in other structures. The Sb or Bi atoms form trigonal pyramids linked to three S atoms whereas Pb_1 and Pb_2 atoms are surrounded by six and nine S atoms, respectively. Therefore, the $CuPbSbS_3$-bournonite is not obtained by substitution of Sb or Bi by Pb in other ternary Cu–Sb–S structures.

In order to obtain the optoelectronic properties we applied the orbital-dependent one-electron potential using the DFT + U formalism described in references [21, 22]. The gaps obtained with U = 0/3/4 eV, are 0.57/1.04/1.22 eV. As a result of the well-known tendency of DFT calculations, the value with U = 0 underestimates the band-gap as compared to the experimental (~1.22 eV [12]). However, the band-gap is closer to the experimental when including an effective Hubbard U = 4 eV in the Hamiltonian.

The analysis of the projected density of states on shell species states (Fig. 2) reveals that the states of the VB and CB edges are derived mainly from the p(S) + d(Cu) and p(S) + p(Sb) + p(Pb) states, respectively.

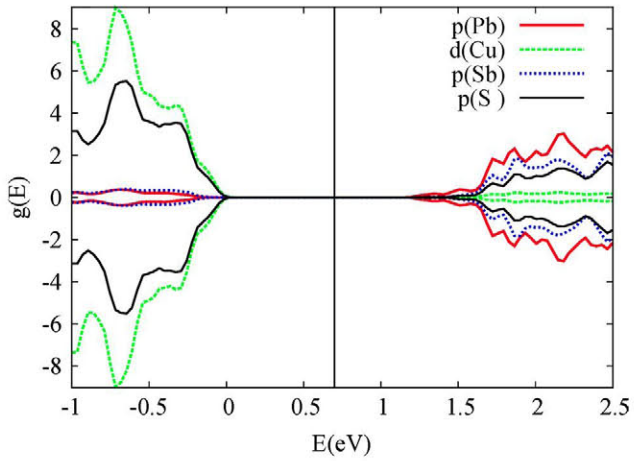

Fig. 2 Projected DOS on shell species states with more contribution to the edges of the VB and the CB. The VB edge has been chosen as the origin of the energy

3.2 Optical properties

The $CuPbSbS_3$-bournonite energy band-gap (E_g ~ 1.22 eV) indicates that this compound may be suitable as a solar radiation absorber in solar cells because the band-gap is closer to the optimal (~41 % at E_g ~ 1.1 eV [14, 16]). Nevertheless, a good candidate for photovoltaic applications must also have a high optical absorption. In order to confirm their application in photovoltaics, we have obtained their optical properties.

Experimentally the reflectivity R and the real refraction index n_I are 26 and 3.1 %, respectively, in the 1.15–1.30 eV energy range [12]. Our results with Ua = 4 eV in this energy range are 25 and 4 % approximately. Therefore, they compare reasonably well with the experimental results. $CuPbSbS_3$-bournonite has a high optical absorption coefficient making it an attractive candidate for use as a light absorber in solar photovoltaic devices. In order to analyze the contribution from different atoms microscopically, we have split the absorption coefficient into inter- (α_{AA}) and intra-species (α_{AB}) contributions in accordance with the methodology section. The results are shown in Fig. 3. The largest contributions are $\alpha_{SS} > \alpha_{PbPb} \sim \alpha_{SbSb} > \alpha_{SbS} \sim \alpha_{SPb}$

According to the former projected PDOS analysis, the greatest contribution to the VB and CB edges are from the p(S) + d(Cu) and p(S) + p(Sb) + p(Pb) states, respectively. Therefore, it could be deduced that the high absorption arises mainly from the $[p(S) + d(Cu)]_{VB} \rightarrow [p(S) + p(Sb) + p(Pb)]_{CB}$ transitions because of a high joint DOS near the semiconductor gap. However, the projected absorption coefficients show that the largest contributions are $\alpha_{SS} > \alpha_{PbPb} \sim \alpha_{SbSb} > \alpha_{SbS} \sim \alpha_{SPb}$.

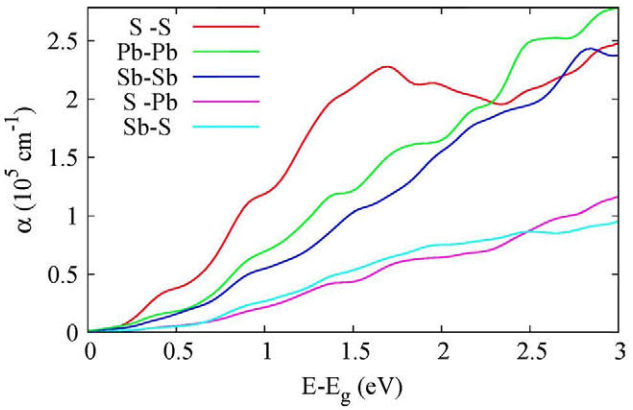

Fig. 3 $CuPbSbS_3$-bournonite absorption coefficient split into atomic contributions. The band-gap energy has been chosen as the origin of the energy

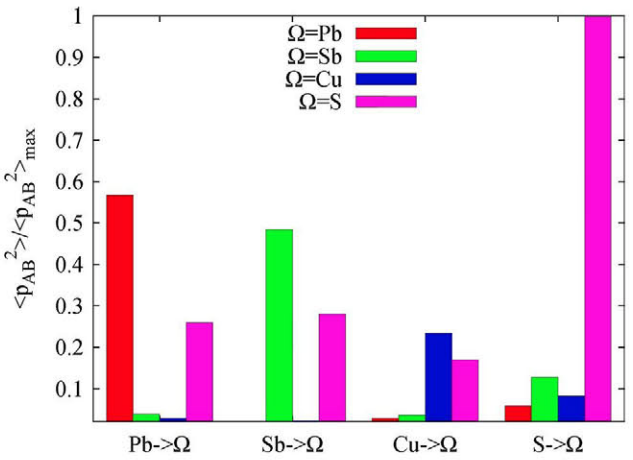

Fig. 4 Mean value of the $p^2_{AB}$for all A → B transitions scaled by the maximum value

We have not taken the transition probabilities into account in the simplified joint DOS. Only if all the momentum operator matrix elements between all bands and all k-points are equal, will the optical properties be proportional to the joint DOS. In order to clarify this aspect we have obtained the mean-value of $\langle p^2_{AB}\rangle$ for all A → B transitions, i.e., $\langle p^2_{AB}\rangle = \sum_{\mu<\lambda} \int d\vec{k} \cdot [f_{\mu,\vec{k}} - f_{\lambda,\vec{k}}]|p^{AB}_{\mu\lambda}|^2$. This is shown in Fig. 4 scaled by the maximum value (S–S in the Figure). From the Figure, the largest values correspond to the A → A intra-species transitions, and with a lower proportion to A → S inter-species transitions. This is in accordance with the order of the split absorption coefficients $\alpha_{SS} > \alpha_{PbPb} \sim \alpha_{SbSb} > \alpha_{SbS} \sim \alpha_{SPb}$, in which the transition probabilities have been considered. Note that the transition probabilities involving Cu, with a large contribution to the VB edge states, are lower than S–S, Pb–Pb, Sb–Sb, S–Sb, and S–Pb. Therefore, the split absorption coefficients involving Cu are small compared with the aforementioned ones.

3.3 Solar cell efficiencies

We have made the assumptions of ideal behavior [14–17] to obtain maximum efficiencies: the cell operates at 300 K, any non-radiative recombination is suppressed, carrier mobilities are infinite (no ohmic losses), and the illumination comes from an isotropic gas of photons from the spectrum of a 5760 K black body reduced by the factor 46,200.

A more important feature, the functional form with respect to the photon energy of the absorption coefficients, has not been paid much attention so far. In part it is due to the assumption that the solar cell absorbs all incident photons above the band-gap. It implies that the absorption coefficient is a step function, zero for energies lower than the energy band-gap, and constant for energies above the band-gap. In this way the dependence is simplified from the absorption coefficient to the band-gap energy. Then the band-gaps are used as an evaluation criterion for solar cell applications [14–17].

Unlike that which is usually done when maximum efficiency is obtained, we have used the absorption coefficients obtained from first principles for several solar concentrations (Fig. 5). As a consequence, the efficiencies depend on the thickness w of the device. From the results in the figure, solar cell devices of just a few microns thick could reach efficiencies close to the maximum overall efficiency (~31 and 41 % for $f_c = 1$ and $f_c \sim 46{,}200$, respectively [7–10]). Therefore, these materials could be very interesting

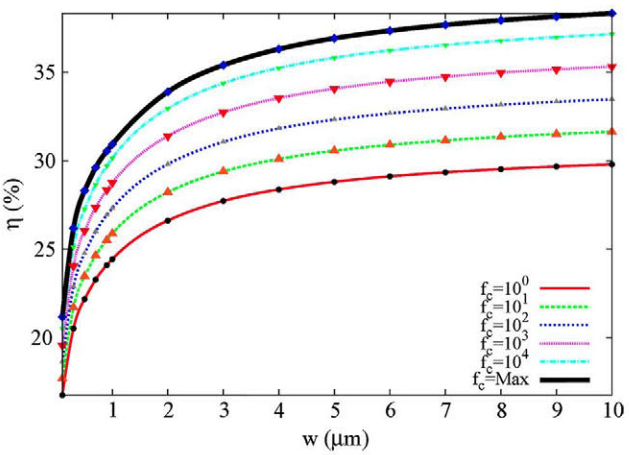

Fig. 5 Efficiency η (%) as a function of the thickness of the cell w for several sun-light concentrations (from $f_c = 1$ sun to maximum concentration f_c = max ~ 46,200 suns, sun units = 1 Kw/m^2). The marks indicate the calculated values. The lines between the marks have been added for visual effect

for photovoltaics when used as an absorbent in solar cell devices.

4 Conclusions

Using GGA + U first-principles density functional theory, we have studied the electronic and optical properties of $CuPbSbS_3$-bournonite. Our theoretical results are in accordance with previous experimental results in the literature. The absorption coefficients have been analyzed in depth, splitting them into inter- and intra-species contributions. The results indicate that the largest contributions to the optical properties are from the S–S > Pb–Pb ~ Sb–Sb > S–Sb ~ S–Pb atomic transitions. We have stressed the deficiencies of a simplified joint DOS analyses where the transition probabilities not taken into account. Finally, its potential as a sunlight absorber in single-gap solar cells has been evaluated from the theoretical absorption coefficients. Solar cells, just a few microns of $CuPbSbS_3$-bournonite thick, could reach efficiencies close to the maximum efficiencies.

Acknowledgments This work has been supported by the National Spanish Project MADRID-PV (S2013/MAE-2780).

References

1. Tablero C (2015) Microscopic analysis and applications of the Cu(Sb, Bi)S2 high optical absorption. J Phys Chem C 119:8857–8863
2. Tablero C (2014) Electronic and optical property analysis of the Cu–Sb–S tetrahedrites for high-efficiency absorption devices. Phys Chem C 118:15122–15127
3. Tablero C (2012) Electronic property analysis of O-doped Cu3SbS3. Sol Energy Mater Sol Cells 104:180–184
4. Van Embden J, Latham K, Duffy NW, Tachibana Y (2013) Near-infrared Absorbing $Cu_{12}Sb_4S_{13}$ and Cu_3SbS_4 nanocrystals: synthesis, characterization, and photoelectrochemistry. J Am Chem Soc 135:11562–11571
5. Yu L, Kokenyesi RS, Keszler DA, Zunger A (2013) Inverse design of high absorption thin-film photovoltaic materials. Adv Energy Mater 3:43–48
6. Jeanloz R, Johnson ML (1984) A note on the bonding, optical spectrum and composition of tetrahedrite. Phys Chem Miner 11:52–54
7. Madelung O (2000) Semiconductors: data handbook. Springer, Berlin
8. Lide DR (ed) (2009–2010) Handbook of chemistry and physics, 90th edn. CRC Press, Taylor and Francis Group, LLC, Boca Raton
9. Rabhi A, Kanzari M, Rezig B (2008) Growth and vacuum post-annealing effect on the properties of the new absorber $CuSbS_2$ thin films. Mater Lett 62:3576–3578
10. Zhou J, Bian G-Q, Zhu Q-Y, Zhang Y, Li C-Y, Dai J (2009) Solvothermal crystal growth of $CuSbQ_2$ (Q = S, Se) and the correlation between macroscopic morphology and microscopic structure. J Solid State Chem 182:259–264
11. Rodríguez-Lazcano Y (2001) thin film formed through annealing chemically deposited Sb_2S_3–CuS thin films. J Cryst Growth 223:399–406
12. Frumar M, Kala T, Horák J (1973) Growth and some physical properties of semiconducting $CuPbSbS_3$ crystals. J Cryst Growth 20:239–244
13. Von Edenharter A, Nowacki W, Tokeughi Y (1970) Verfeinerung der Kristallstruktur von Bournonit $[(SbS_3)_2|Cu_2^{IV}Pb^{VII}Pb^{VIII}]$ und von Seligmannit $[(AsS_3)_2|Cu_2^{IV}Pb^{VII}Pb^{VIII}]$. Z. Zeitschrift für Kristallographie 131:397–417
14. Luque A, Martí A (2003) Theoretical limits of photovoltaic conversion. In: Luque A, Hegedus S (eds) Handbook of photovoltaic science and engineering. Wiley, London
15. Würfel P (2005) Physics of solar cells. From principles to new concepts. Wiley, London
16. Green MA (2006) Third generation photovoltaics. Advanced solar energy conversion. Springer, Berlin
17. Brown AS, Green MA (2002) Impurity photovoltaic effect: fundamental energy conversion efficiency limit. J Appl Phys 92:1329–1336
18. Kohn W, Sham LJ (1965) Self-consistent equations including exchange and correlation effects. Phys Rev 140:A1133–A1138
19. Soler JM, Artacho E, Gale JD, García A, Junquera J, Ordejon P, Sánchez-Portal D, SIESTA code (2002) The SIESTA method for ab initio order-N materials simulation. J Phys Condens Matter 14:2745
20. Anisimov I, Zaanen J, Andersen OK (1991) Band theory and Mott insulators: Hubbard U instead of Stoner I. Phys Rev B 44:943
21. Tablero C (2008) Representations of the occupation number matrix on the LDA/GGA + U method. J Phys Condens Matter 20:325205
22. Tablero C (2009) Effects of the orbital self-interaction in both strongly and weakly correlated systems. J Chem Phys 130:054903
23. O'Regan DD, Payne MC, Mostofi AA (2011) Subspace representations in Ab initio methods for strongly correlated systems. Phys Rev B 83:245124
24. Grisolía M, Rozier P, Benoit M (2011) Density functional theory investigations of the structural and electronic properties of $Ag_2V_4O_{11}$. Phys Rev B 83:165111
25. Perdew JP, Burke K, Ernzerhof M (1996) Generalized gradient approximation made simple. Phys Rev Lett 77:3865
26. Perdew JP, Burke K, Ernzerhof M (1997) Phys Rev Lett 78:1396
27. Troullier N, Martins JL (1991) Efficient pseudopotentials for plane-wave calculations. Phys Rev B 43:1993
28. Kleinman L, Bylander DM (1982) Efficacious form for model pseudopotentials. Phys Rev Lett 48:1425
29. Bylander DM, Kleinman L (1990) 4f resonances with norm-conserving pseudopotentials. Phys Rev B 41:907
30. Sankey OF, Niklewski DJ (1989) Ab initio multicenter tight-binding model for molecular-dynamics simulations and other applications in covalent systems. Phys Rev B 40:3979